

This article was downloaded by: [Tomsk State University of Control Systems and Radio]

On: 23 February 2013, At: 08:11

Publisher: Taylor & Francis

Informa Ltd Registered in England and Wales Registered Number: 1072954

Registered office: Mortimer House, 37-41 Mortimer Street, London W1T 3JH, UK



Molecular Crystals and Liquid Crystals

Publication details, including instructions for authors and subscription information:

<http://www.tandfonline.com/loi/gmcl16>

Thermal Radiography Utilizing Liquid Crystals

R. D. Ennulat^a & J. L. Fergason^b

^a U.S. Army Electronics Command, Night Vision Laboratories, Fort Belvoir, Virginia

^b Liquid Crystal Institute, Kent State University, Kent, Ohio

Version of record first published: 28 Mar 2007.

To cite this article: R. D. Ennulat & J. L. Fergason (1971): Thermal Radiography Utilizing Liquid Crystals, *Molecular Crystals and Liquid Crystals*, 13:2, 149-164

To link to this article: <http://dx.doi.org/10.1080/15421407108084960>

PLEASE SCROLL DOWN FOR ARTICLE

Full terms and conditions of use: <http://www.tandfonline.com/page/terms-and-conditions>

This article may be used for research, teaching, and private study purposes. Any substantial or systematic reproduction, redistribution, reselling, loan, sub-licensing, systematic supply, or distribution in any form to anyone is expressly forbidden.

The publisher does not give any warranty express or implied or make any representation that the contents will be complete or accurate or up to date. The accuracy of any instructions, formulae, and drug doses should be independently verified with primary sources. The publisher shall not be liable for any loss, actions, claims, proceedings, demand, or costs or damages

whatsoever or howsoever caused arising directly or indirectly in connection with or arising out of the use of this material.

Thermal Radiography Utilizing Liquid Crystals†

R. D. ENNULAT

U.S. Army Electronics Command
Night Vision Laboratories
Fort Belvoir, Virginia

and

J. L. FERGASON‡

Liquid Crystal Institute
Kent State University
Kent, Ohio

Abstract—A thermal imaging system using cholesteric liquid crystals has been designed and built which utilizes the extreme temperature sensitivity of cholesteryl oleyl carbonate. Theoretical considerations for the design and the operating conditions of the device are given. The experimental results indicate that the limitations on such a device are primarily due to the finite film thickness required for scattering by the cholesteric liquid (on the order of ten micrometers). This system was able to image 0.2°C with a limiting resolution of one line pair per millimeter. Improved lighting for direct viewing of the liquid crystal film should result in a sensitivity of about 0.02°C .

Introduction

Thermal radiography deals with the registration of radiation inherently emitted by physical objects due to differences in emissivity and/or temperature.⁽¹⁾ Thermal imaging systems are the most useful and versatile radiographic devices because they convert the invisible image formed by this infrared radiation into a visible replica. Thus the observer is able, for example, to see at night without extraneous illumination, to find certain structural faults in work pieces indicated by small temperature differences, to detect overheated components in electronic circuitry, and to test the blood circulation at the surface

† Presented at the Third International Liquid Crystal Conference in Berlin, August 24-28, 1970.

‡ Work performed while employed at the Westinghouse Research Laboratories, Pittsburgh, Pennsylvania.

of the human body and the malignancy of tumors. To date, widespread application of this powerful technique is restricted by the high cost of present infrared imaging devices. In the following we will describe and discuss a relatively simple, inexpensive thermal imaging device invented by Ferguson, Garbuny and Vogl,⁽²⁾ using as a transducer a thin film of a cholesteric liquid crystal.

Concept of Thermal Imaging Device

This thermal imaging device utilizes the temperature dependence of the light selectively reflected by the plane texture of a cholesteric liquid crystal. Figure 1 shows the spectral profiles of the light selectively reflected by regions of temperature T_A and T_B of the cholesteric film. If this film is illuminated with monochromatic light of wavelength λ_0 , the region of temperature T_A has a much lower reflected intensity for light of wavelength λ_0 than the surrounding region of temperature T_B . Thus the observer perceives regions of different temperatures as regions of different brightness.

Figure 2 shows the schematics of a thermal imaging device based on this conversion principle. The infrared image of the scene is focused on the absorbing side of a membrane and converted by absorption into the corresponding heat pattern. Thermal conduction

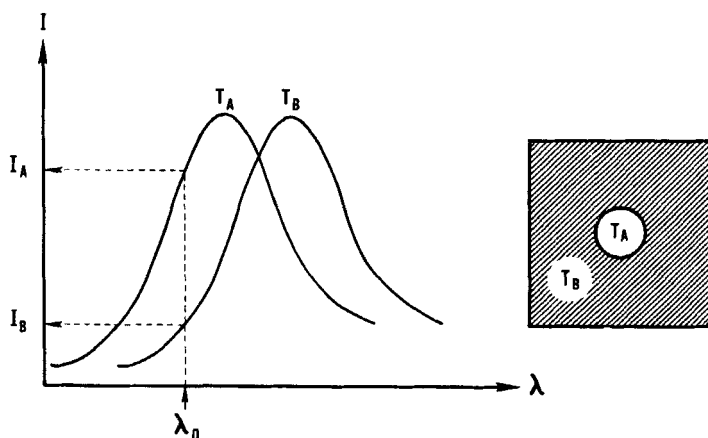


Figure 1. Conversion Principle.

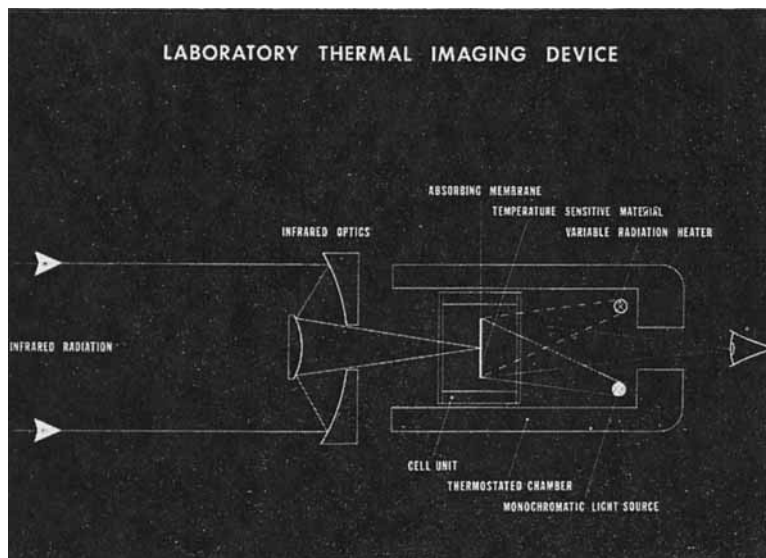


Figure 2. Laboratory Thermal Imaging Device.

establishes an equivalent temperature pattern in the cholesteric liquid crystal, deposited on the other side of the membrane. Because of the temperature dependent selective reflectivity of the liquid crystal, this temperature image—and thus the original infrared image—is made visible by illumination with monochromatic light. To keep the liquid crystal at the proper operating temperature the sensing layer is enclosed in a coarsely temperature controlled chamber. A radiation heater provides fine control of the operating temperature. By varying the output of the radiation heater desired temperature levels of the temperature image in the liquid crystal can be brought into the selective reflection region and can thus be made visible. This capability and the extreme non-linearity of the temperature dependence of the selective reflection (i.e. its cut-off characteristics) are essential to suppress the unwanted effect of high background radiance of the scene without reducing the effect of the radiance coming from objects of interest. As we will see temperature differences of 0.2°K in the scene can be detected against a background of 300°K . It is very difficult to achieve such a performance with other non-scanning infrared to visible image converters.

Theoretical Consideration

To assess the potential of this thermal imaging principle we determine the minimum observable temperature difference as a function of a parameter characterizing resolution.

Figure 3 shows the parameters responsible for the radiation balance of the transducer. The radiation, emanating from background of temperature T_s and object of temperature $T_s + \Delta T_T$, is attenuated by a factor $t_A(\lambda)$ due to atmospheric absorption and focused by an

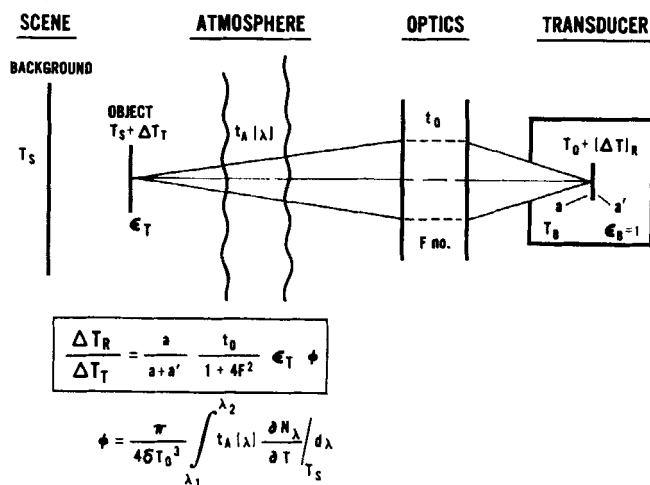


Figure 3. Radiation Balance of Transducer.

optics, characterized by an attenuation factor t_0 and an f /number F , onto the transducer film. The latter is contained in a totally absorbing box admitting external radiation only through the optics. In the following we will treat ϵ_T , t_0 , a , and a' as constants. This will simplify the problem significantly and still cover most of the practical cases.† For uniform background of temperature T_s the sensing layer assumes a “reference temperature” T_0 . For an object of temperature $T_s + \Delta T_T$ in the scene, we obtain a corresponding pattern

† We assume in particular that the emissivities a and a' of the sensing layer are practically independent of the angle of incidence. The problem can be readily solved without those assumptions but the outcome will not contribute to the general understanding.

of temperature $T_0 + \Delta T_R$ on the membrane. If no lateral heat conduction occurs in the transducer film, we obtain according to Weihe⁽³⁾ the relation†

$$\Delta T_R = \frac{a}{a+a'} \frac{t_0}{1+4F^2} \epsilon_T \phi \Delta T_T$$

$$\phi = \frac{\pi}{4\sigma T_0^3} \int_{\lambda_1}^{\lambda_2} t_A \left. \frac{\partial N_\lambda}{\partial T} \right|_{T_s} d\lambda \quad (1)$$

where $N_\lambda(T)$ is the spectral radiance, σ the Stefan-Boltzmann constant.

ϕ , a quantity strongly dependent on the water content, can be determined from tabulated data.⁽⁴⁾ For example, for the 8 to 14 μm wavelength region, a most suitable "atmospheric window" for our device, ϕ is approximately $\frac{1}{2}$ if the airpath contains 0.7 mm precipitable water and about $\frac{1}{3}$ if the airpath contains 17 mm precipitable water⁽³⁾.

Next we address the influence of lateral heat conduction on the temperature distribution of the membrane. This problem can be solved in general for all radiance patterns imposed on the membrane if the heat conduction equation is linear, that is if the superposition principle is valid. We estimate that this is the case with sufficient approximation if the temperatures in the scene and of the transducer membrane and its inclosure differ by less than twenty percent. It is practical from the theoretical point of view to construct solutions of the heat conduction equation by superposition of temperature distributions obtained for sinusoidal radiance input. Since we did not have sources of sinusoidal radiance, we tested the thermal imaging device with bar pattern images (Fig. 4, upper curve). By reducing the temperature amplitude to the minimum observable level, we actually observe only the radiance contribution of the fundamental (Fig. 4, lower curve) as the following expression⁽⁵⁾ shows:

$$\Delta T_{pp} = \frac{4}{\pi} \Delta T_R \sum \frac{(-1)^n}{(2n+1)[1+(2n+1)^2 4\pi^2 (L_0/L)^2]} \approx$$

$$\frac{4}{\pi} \Delta T_R \frac{1}{1+4\pi^2 (L_0/L)^2} \quad L_0 = \sqrt{\frac{k_1 h_1 + k_2 h_2}{4(a+a')\sigma T_0^3}} \quad (2)$$

† Since the distance of the objects from the optics is always more than 10 times the focal length, the effect of the magnification was neglected.

The characteristic length L_0 governing the resolution of the layer, depends on the thicknesses h_1 , h_2 and the thermal conductivities k_1 , k_2 of membrane and liquid crystalline film respectively.

Finally we have to relate the temperature differences in the liquid crystal film to the corresponding perceivable brightness differences. Figure 5 shows the membrane brightness as a function of temperature. The brightness level consists of a constant background brightness αI_{\max} caused by specular reflections and scattering of the illuminating light and of the temperature dependent contribution I

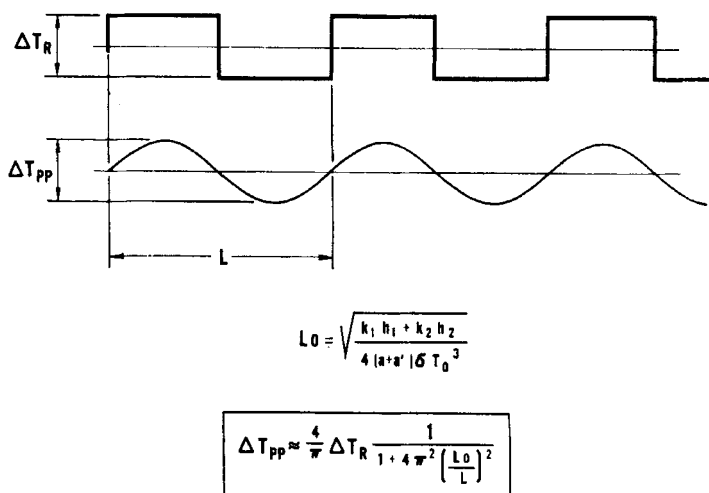
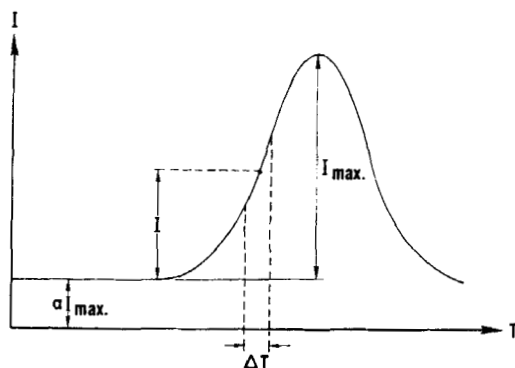


Figure 4. Bar Pattern Image.

due to selective reflection. For a bar pattern image of amplitude $\Delta T/2$ we obtain a corresponding spacial brightness variation $\Delta I/2$ superimposed on the average brightness level $\alpha I_{\max} + I$. Since the human eye responds to the contrast $\Delta I/I$ rather than to the brightness differences ΔI itself, we need to know the threshold contrast K_{\min} for the determination of the minimum observable temperature difference. Considering that ΔI is equal to $I \Delta T C$, where C is the temperature coefficient of the brightness and considering that the maximum temperature coefficient occurs at the inflection points of the spectral response curve of cholesteryl oleyl carbonate at approxi-



$$\text{THRESHOLD CONTRAST} \quad K_{\min.} = \left| \frac{\Delta I}{I} \right|_{\min.}$$

$$\text{MAXIMUM TEMP. COEFF.} \quad C_{\max.} = \frac{\Delta I}{1/2 I_{\max.}} \frac{1}{\Delta T}$$

$$\Delta T_{\min.} = \frac{K_{\min.}}{C_{\max.}} (1 + 2\alpha)$$

Figure 5. Minimum Detectable Temperature Difference.

mately $I = \frac{1}{2} I_{\max.}$ ⁽⁶⁾ we obtain for the minimum observable temperature difference

$$\Delta T_{\min} = \frac{K_{\min}}{C_{\max}} (1 + 2\alpha) \quad (3)$$

Notice the degrading influence of the background brightness I_{\max} on this quantity. By combining the Eqs. (1), (2) and (3) we obtain for the minimum observable temperature difference $(\Delta T_T)_{\min}$ in the scene

$$(\Delta T_T)_{\min} = A \left(1 + 4\pi^2 \left(\frac{L_0}{L} \right)^2 \right) \quad (4)$$

$$A = \frac{\pi \Delta T_T}{4 \Delta T_R} \frac{K_{\min}}{C_{\max}} (1 + 2\alpha) \quad (4a)$$

where the pattern wavelength L is measured on the membrane. In the following we will utilize this relation to appraise experimentally the potential of this thermal imaging approach.

Experimental Studies

The experimental studies were conducted with a device designed to demonstrate the feasibility of the thermal imaging approach and

to permit studies of cholesteric liquid crystals, having widely differing operating temperatures. This test device, designed by Hansen and Ferguson of the Westinghouse Corporation, is shown in Fig. 6. It consists of a reflective optics, a thermoelectric thermostat and of a thermostated chamber containing illuminator, radiation heater and the evacuated cell unit enclosing the transducer film. The optics, originally designed for a different purpose, has five reflective elements. Its optical axis in the image space is at right angles to that of the object space and its long back focal length permits the focusing of the image about 5 cm inside the thermostated enclosure. The thermostat generates thermostated water heated or cooled by a thermoelectric converter and pumps it through grooves of the chamber. A contact thermometer mounted in a water reservoir permits adjustment and control of the water temperature. A circular shaped

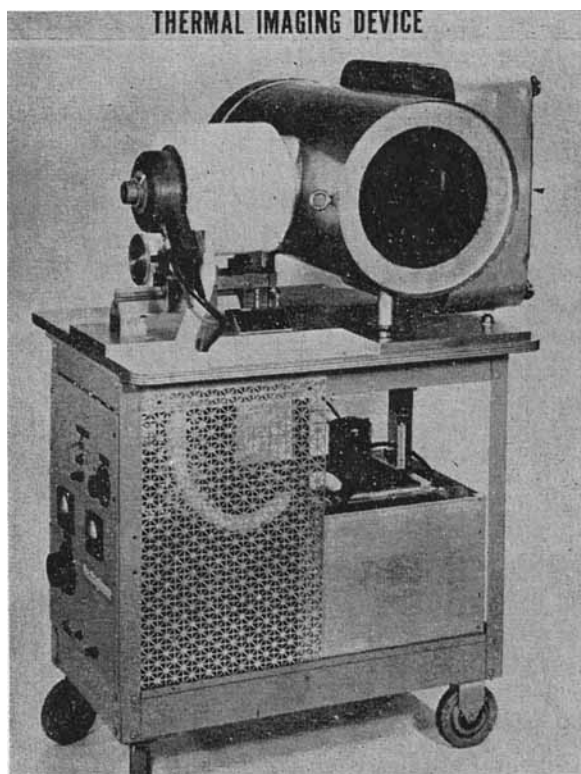


Figure 6. Laboratory System.

He gas discharge lamp and a radiation heater, consisting of a ring of 8 lightbulbs, blackened to eliminate visible light, are mounted in the plate closing the chamber towards the observer. The cell unit, shown in Fig. 7, is a blackened brass cylinder closed on one side by a germanium window for the infrared input and on the other side by an ordinary glass window to admit viewing light and heater radiation. The transducer membrane is suspended in the inside with the infrared absorber directed towards the germanium window. The cell unit is evacuated by a mechanical pump to prevent the degradation of the image resolution due to heat conduction through the surrounding air. A liquid nitrogen cold trap prevents the contamination of the liquid crystal film due to backstreaming pump oil.

Preparation of Transducer Membranes

To obtain the highest resolution (i.e. the smallest characteristic length L_0) and the smallest observable temperature difference ΔT_{\min} the transducer film must be as thin as possible and the selective reflection of the liquid crystal must be large in intensity and narrow

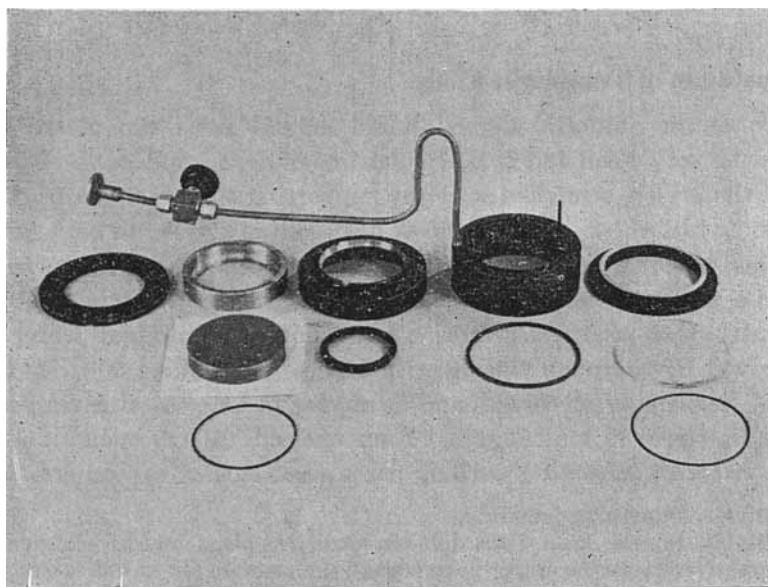


Figure 7. Cell Unit.

in its spectral response. This requires almost complete alignment of the plane texture and a certain optimum thickness so that the light can interfere with a sufficient number of repeat distances of the liquid crystal structure. We found that liquid crystal films thinner than $5\mu\text{m}$ (i.e., roughly 10 times the wavelength of light) yield insufficient intensity of selectively reflected light while layers thicker than $20\mu\text{m}$ exhibit selective reflection against a high background of diffuse light. (The latter is apparently caused by the scattering of light on small unaligned regions of the plane texture.) Thus the optimum thickness must be somewhere between 5 and $20\mu\text{m}$. The exact value depends on the particular liquid crystal and on the properties of the supporting substrate. The latter should be thin as compared to the liquid crystal film and should induce a well aligned plane texture spontaneously. Furthermore, to obtain a stable film the liquid crystal should wet the support sufficiently. Since the problem associated with these requirements can only be solved with considerable effort, we had to restrict ourself to an empirical selection of substrates. We found that Mylar† membranes of about $6\mu\text{m}$ thickness provided the best substrates‡ and that the optimum thickness of liquid crystal must be between 10 and $15\mu\text{m}$.

Preparation of Transducer Films

To obtain uniform aligned liquid crystal films the membrane must be very clean and in particular free of grease and dust. Therefore the Mylar, stretched over the supporting ring, is first rinsed in running tap water. Then a dab of detergent is applied to both sides, rubbed thoroughly but gently (to avoid stretching) on both surfaces with a moist cotton swab and rinsed off with tap water and subsequently with distilled water. Afterwards the residual water is removed by thorough rinsing with hexane, containing 30% chloroform, benzene or methanol, and by drying in an oven at a temperature between 80 and 100°C . Then one side of the membrane is sprayed with infrared absorbing paint consisting of carbon granules

† Mylar, Dupont trademark.

‡ Mylar, thinner than $6\mu\text{m}$ did not align the plane texture sufficiently apparently because the proper polar surface regions were not as well developed as for $6\mu\text{m}$ material. However, no effort was made to develop extremely thin Mylar membranes specifically for this application.

(average size about $2\mu\text{m}$) and of an organic binder. To obtain favorable thermal properties the amount of binder is reduced to the minimum.

The liquid crystal film can be applied by spreading or by spraying. In the spreading method about 0.1 ml of a 10 to 20% solution of liquid crystal is deposited with an eye dropper in the center of a horizontal membrane. The liquid rapidly spreads and evaporates leaving a thin, uniform area of liquid crystal behind, surrounded by an enclosing thicker rim. The latter is caused by the gradual increase of concentration and by the reduction of speed of spreading of the solution. The uniform center part is used as the sensing layer. Depending on the particular liquid crystal and on the ambient temperature a proper solvent mixture must be selected to adjust solubility and speed of spreading. For example petroleum ether or pentane should be used for temperatures of 25°C or below, while ligroin is a better solvent for higher temperatures. To obtain the proper film thickness the solvent should contain between 10 and 20% liquid crystal.

Better control of thickness and uniformity is obtained by a spraying method, suggested by F. M. Schaer. Using an ordinary artist air brush with the finest nozzle, a mixture of 20% liquid crystal and 80% chloroform is sprayed on the membrane using as a carrier gas dry nitrogen at a pressure of 50 p.s.i. By spraying at a distance of about 30 cm a skilful operator can obtain very uniform membranes. Better results requiring less operator skill are obtained with a Zicon Spray Gun (Chemtronic, Mount Vernon, New York) which uses as a carrier gas superheated freon at a pressure of about 50 p.s.i. A mixture of 10% liquid crystal and cyclohexane (chloroform evaporates too fast) is sprayed with the finest nozzle at a distance of 15 to 20 cm.†

The spraying methods and to a lesser extent the spreading method have to be applied in a dry atmosphere, since the gas expanding from the nozzle‡ and the solvent evaporating from the film lower the temperature. If the temperature of the liquid crystal drops below the dew point the moisture of the atmosphere precipitates on the

† According to the manufacturer this gun can deposit films as thin as $0.5\mu\text{m}$ with a thickness variation of less than $\pm 10\%$.

‡ The temperature of the expanding gas at the nozzle can be as low as 0°C !

sensing layer and appears as a veil of little droplets. This gives the layer the appearance of an orange peel. To avoid this undesirable non-uniformity and the deposition of dust particles, all critical operations such as final cleaning of the membrane, application of liquid crystal, and assemblage of the cell unit are performed in a bag of dry, ultra clean air.

The uniformity of the cholesteric film was qualitatively assessed in the thermal imaging system by capping the entrance stop of the optics with a metal plate of ambient temperature. By changing the average temperature of the membrane with the radiation heater and by rotating the whole cell unit one obtains a qualitative impression of uniformity. If the pattern of the selectively reflected light is invariant against rotation at various temperature levels, the centrosymmetric pattern is caused by the radiation field of the optical system (which has rotational symmetry) and not by non-uniformities of the membrane.

Experimental Tests

To assess this thermal imaging approach we have to distinguish between the limiting factors inherent of our particular device and those characteristic of the liquid crystal sensing layer. We made this distinction by directly determining the temperature difference on the membrane caused by a given temperature difference in the scene and by determining the minimum observable temperature differences of bar pattern images in dependence of pattern wavelength.

Two large black plates of equal emissivity ($\epsilon \approx 1$) but differing in temperature by ΔT_T were placed in the scene and imaged onto the sensing layer. Since the lateral dimensions of the associated images were large as compared to the characteristic length L_0 of the sensing layer, their temperature difference ΔT_R in the center was not noticeably affected by the lateral heat conduction. We adjusted the temperature difference T_T in the scene so that these images exhibited maximum selective reflection at the He lines $501.5 \text{ m}\mu$ and $587.5 \text{ m}\mu$. This event was precisely determined with a spectrophotometer of $0.6 \text{ m}\mu$ resolution. Then we placed a piece of this sensing layer in a thermostated oven and determined with the aid of a photometer the

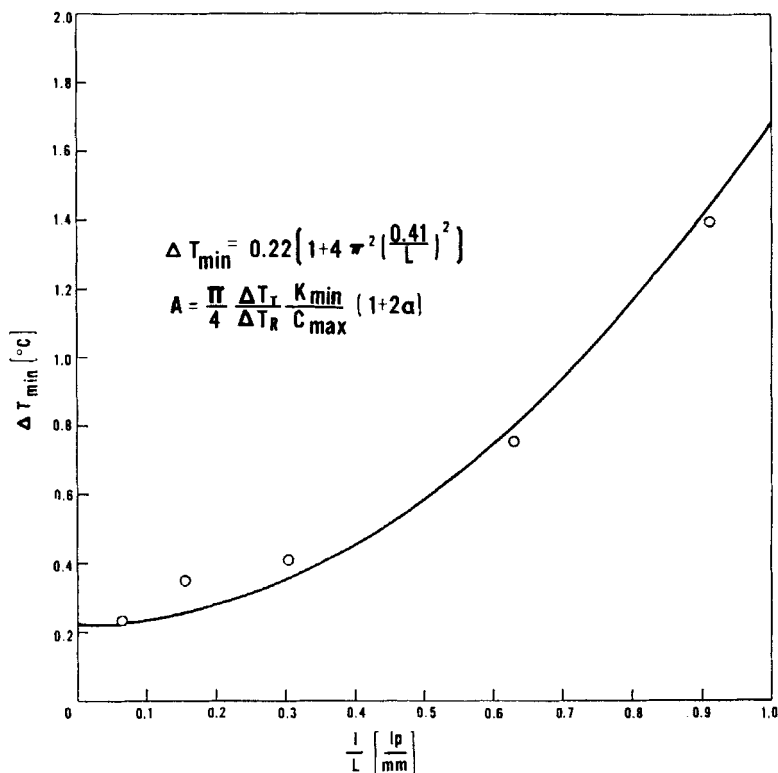
temperature associated with the respective wavelengths. Thus we found that a temperature difference of $\Delta T_T = 11.5^\circ\text{C}$ in the scene corresponds to a temperature difference $\Delta T_R = 0.17 \pm 0.02^\circ\text{C}$ on the membrane.

This result indicates that the obscuration of the optics and the losses caused by the five reflective elements and by the germanium window reduce the received radiation by 85%!

The resolution test was made with the following set-up. A comb-shaped bar pattern cut out of a 0.6 cm thick aluminum plate was placed in front of a thick copper plate (0.6 cm thick), the temperature of which was adjustable. Both pattern and background plate were thermally insulated from each other and their front faces were coated with paint of emissivity close of one. The temperature difference between those two plates was determined with a copper-constantan thermocouple within $\pm 0.02^\circ\text{C}$. To facilitate the tests the copper plate and the attached electrical heater were heat sunked.[†] By increasing or reducing the heater current we could impart a temperature drift slow enough to prevent thermal lags and yet fast enough to reduce testing time. Furthermore, we could adjust the background temperature level below and above the bar pattern temperature, which was always approximately at room temperature. The tests were conducted by two persons, one of them adjusting and measuring the temperature and the other one viewing the bar pattern image and indicating its appearance or disappearance. By changing the temperature in one direction one obtained the minimum observable temperature difference for, say, a background hotter than the bar pattern and subsequently for the reverse case. As expected for negligible thermal lags both minimum observable temperatures were equal within the uncertainties of this subjective measurement of approximately $\pm 20\%$.

Figure 8 presents the results of this test and the closest fit of the theoretical curve (Eq. (4)), which determined the characteristic length $L_0 = 0.41$ mm and the factor $A = 0.22$ ($^\circ\text{C}$). Substituting into Eq. (2) for L_0 the known values $k_1 = 8.96 \times 10^{-5}$ cal/sec cm $^\circ\text{C}$ and $h_1 = 6 \mu\text{m}$ for Mylar, $k_2 = 2.9 \times 10^{-4}$ cal/sec cm $^\circ\text{C}$ for the liquid

[†] We used a 0.5 cm thick layer of transformer oil as a thermal barrier between the copper plate and the aluminum tank containing ice and water. Because of leaks we replaced the oil by silicon rubber.



MINIMUM OBSERVABLE TEMPERATURE DIFFERENCE IN DEPENDENCE OF RESOLUTION

Figure 8. Limit of Resolution.

crystal,[†] and setting $T_0 = 300^\circ\text{K}$ we obtain for the thickness h_2 of the liquid crystal $10\mu\text{m}$, i.e., a value within the expected range of thickness. According to Eq. (4a), the value of A permits the determination of the magnitude of the threshold contrast K_{\min} . By considering that $\Delta T_T/\Delta T_R = 68$, $C_{\max} = 100$ ($^\circ\text{C}$) for cholesteryl oleyl carbonate⁽⁶⁾, and $\alpha = 3$ (as determined by a simple photometric test) we obtain $K_{\min} = 0.06$. This value deviates by a factor of 3 from the literature value⁽⁷⁾ reported for 0.05 linepairs per millimeter, i.e. for the resolution at which $\Delta T_{\min} \approx A$. However, this discrepancy is not large if one considers that K_{\min} depends strongly

[†] We measured k_2 by determining the heat current through and the temperature drop across a liquid crystal film.

on the human observer, the state of adaptation of the eye, and of other quantities not controlled in our experiment.

Figure 9 shows the thermal image of a person taken at a distance of about 4 m against a room temperature background. Since we could not fix the slowly drifting temperature of the membrane during the exposure time, the image quality of these photographs is quite inferior to that of the directly observed image. The features of a hand suddenly raised are sharp within about 4 to 5 seconds. This indicates a thermal time constant of the order of a few seconds, which is typical for radiation cooled transducers.

These experiments show that the performance of this thermal imaging device is severely limited by the high background luminance $(\alpha + \frac{1}{2})I_{\max}$ of the viewing light and by the efficiency of the optics. If α would be reduced from 3 to 0.1—and this can be done by using collimated, linear polarized viewing light—and if the optics would transmit at least 30% (instead of 15%) of the received radiation,

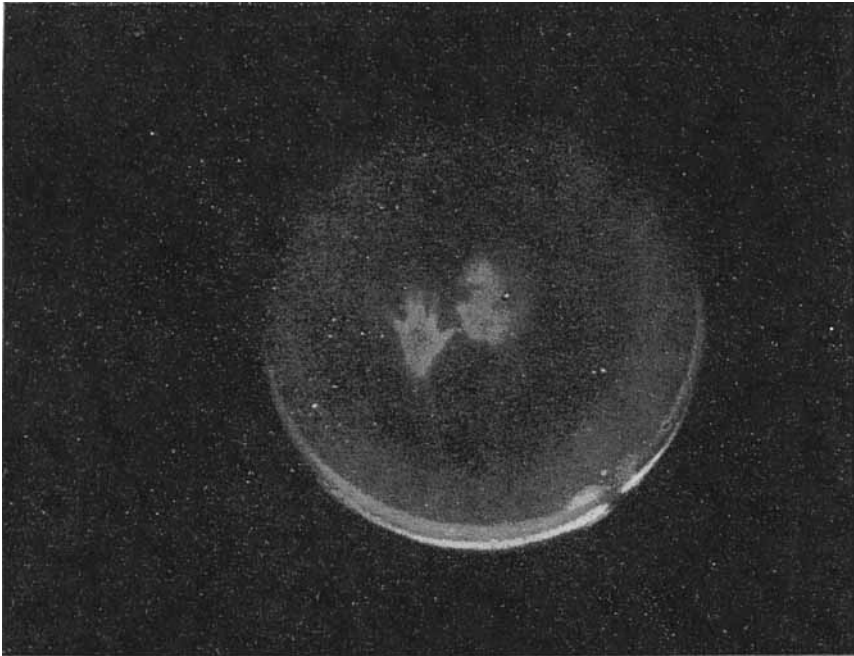


Figure 9. Thermal Image of a Person.

the minimum observable temperature difference in the scene would drop from 0.2°C to less than 0.02°C .

It can be concluded that this thermal imaging approach is capable of detecting temperature differences as small as 0.02°C . However, for fundamental reasons it is severely limited in spacial resolution to the order of a line pair per millimeter and to a time constant of the order of a second, because the thickness of liquid crystalline layers cannot be reduced substantially below $10\mu\text{m}$ without adversely affecting the selective reflectivity.

REFERENCES

1. See for example, Infrared Imaging Issue, Applied Optics, Vol. 7, September 1968.
2. Ferguson, J. L., Vogl, Th. and Garbuny, M., Patent 3,114,836 (U.S.).
3. Weihe, W. K., *Proc. IRE*, **47**, No. 9, p. 1593 (1959).
4. Taylor, J. H. and Yates, H. W., Naval Research Report No. 4759, May 11 (1956).
5. Jones, R. C., Polaroid Corp., Cambridge, Mass., Interim Tech. Report No. 188, Contract DA-44-009-ENG-1727.
6. Ennulat, R. D., to be published in Proceed. Third Liq. Cryst. Conf., 1970.
7. DePalman, J. J. and Lawry, E. M., *Journal Opt. Soc. Am.* **52**, No. 3, p. 328 (1962).